

Synergistic effect of graphene oxide and colloidal nano-silica on the microstructure and strength properties of fly ash blended cement composites

Kalaiselvi Subramani¹ , Arun Kumar Ganesan²

¹Sona College of Technology, Department of Civil Engineering, Salem, India.

²Government College of Engineering, Department of Civil Engineering, Thanjavur, India.

e-mail: skalaiselvi1515@gmail.com, arun_8112005@yahoo.com

ABSTRACT

Cement concretes are widely used and very effective in the construction industry. Micro-scale problems such as porosity, micro-cracks, etc. Many researchers have done research work globally to address this issue. This research investigation also addresses this by using colloidal nano-silica along with Graphene oxide (GO) particles in fly ash-based cement compounds. The change in the behaviour of cement matrix experimentally observed with 10% replacement of FA with cement, 2.5% replacement of Nano-silica with cement, and GO of variable dosage in this research investigation, GO as additive of dosages 0.02%, 0.03%, 0.04%, 0.05%, and 0.06% by mass of cement has been used. GO and Nano-silica were sonicated for 30 minutes to get uniform dispersion of nanoparticles. The material characterization and cement blended composite characterization has been performed using Energy-dispersive X-ray analysis, Scanning Electron Microscopy, X-Ray diffraction, and Fourier transform infrared tests. From the Test results, it is found that the addition of 0.03% of GO is the optimum dosage of the cement composites. It is observed that GO+NS with FA affects the overall hydration process of the cement composites. GO, and NS fills the pores, causing a reduction in pore volume and promoting the more compact and dense microstructure.

Keywords: Graphene oxide (GO); Nano silica (NS); Fly ash (FA); SEM; EDX; XRD; FTIR.

1. INTRODUCTION

Cement concretes are widely used and very effective in the global construction industry. This includes important structures such as bridges, tunnels, and offshore and onshore structures. The Strength and serviceability of the structure should be ensured. Since cement concrete is highly heterogeneous, it is challenging to meet the required mechanical properties. Cement concrete has low tensile Strength as it behaves in quasi-brittle nature. Moreover, the resistance to crack propagation is meagre. The external reinforcement with ductile materials will enhance the behaviour of cement concrete on its macro scale. This will not help to improve the micro-scale problems such as porosity, development of micro-cracks, etc. These micro-level problems should be addressed to enhance the overall behavior of cement concrete. One of the best solutions for this problem is the use of Nanomaterials (10–9) like Nano-silica, Nano-clay, Carbon-Nanotube (CNT), Carbon-Nanofiber (CNF) [1,2], and so on.

Nano materials are categorized as zero dimensional, one-dimensional, and two-dimensional, depending on their atomic chain nature. The zero dimensional particles, such as nano-silica, can arrest the development of cracks as they act only as the filling material and fill the pores. One-dimensional particles such as CNTs exhibit stout Van Der Waal's force. These particles have good dispersion for better performance. Two dimensional particles such as Graphene Oxide (GO) have been considered the prime additive in this study to analyse its performance. As the particle size decreases, the surface area of the same increases. This huge surface area of nanoparticles chains the formation of nucleation sites for hydration of cement which in turn increases the degree of hydration [3–6]. GO Nano sheets quickens the hydration of cement to produce flower-like hydration crystal, leading to an increase in the strength properties of the cement composites [3]. The incorporation of an optimum quantity of GO blended cement compounds improves the microstructure properties of the cement compounds [7]. Presence of oxygen containing functional groups consisting of hydroxyl and carboxyl carbonyl groups at the edges causes uniform dispersion in water to occupy the micro pores, increases the heat of hydration and

Table 1: Authors and their contributions.

AUTHORS	SPECIMEN	DESCRIPTION	COMPRESSIVE STRENGTH
WANG <i>et al.</i> [16]	GO+Fly ash	Enhancement of Strength due to drop of pores in the composite.	25% increase due to reinforcement of 0.01% (wt) GO and 5% (wt) FA
PRABAVATHY <i>et al.</i> [17]	rGO–Cement	The presence of needle-shaped hydration crystals forms a dense and compact structure.	44% increase due to reinforcement of 0.1% (wt) rGO
LEE <i>et al.</i> [18]	GO (2D - Nano Structure)	The formation of dense and compact microstructure improves the compressive strength.	22.7–45.5% enhancement in Strength was found by the combination of 0.03% (wt) GO
LI <i>et al.</i> [19]	GO	Compressive Strength was improved due to the alteration of pore structure.	A 6% rise in Strength was found by the addition of 0.03% (wt) GO
WANG <i>et al.</i> [20]	GO+FA	Speeding up of secondary hydration, reduction in the volume of pores, and modification of CH crystal enhances the rise in durability and mechanical properties of the composite	8.9% increase in compressive Strength at 0.03% of GO with 10% of FA.

enhances the properties of the cementitious compounds [8–10]. The Hydrophilic nature of GO enables the particles to disperse uniformly in water. Also, GO has many active sites for tying together organic molecules and other functional groups [11].

Oxygen functional groups in GO can potentially reduce van der Waals forces and increase electrostatic repulsion between GO sheets., making it simpler for the material to diffuse in water [12]. The interfacial bonding of the cementitious materials could be enhanced by the active functional groups. Due to these benefits, GO has recently received a lot of attention and is commonly employed in a variety of composites made of cement [13]. The existence of C3S in GO Nano sheets alters the morphology of the C-S-H gel in cement. GO Nano sheets act as a 2D platform for the growth of Calcium silicate hydrate products with plate-like morphology that supports the formation of the dense and compact nanostructure [14]. GO blended cement composites refine the microstructure by controlling the hydration crystal's alignment. The enhanced hydration on the active sites of GO accelerates the chemical composition of inorganic crystalline phases of hydration products [15]. Table 1 lists some of the experimental works contributed by the researchers for strength behaviours around the globe.

The objectives of incorporating additional materials in concrete include improved Strength, Enhanced Workability, Enhanced Resistance to Chemical Attack, Control of Shrinkage Cracking, Tailoring Properties of Nano materials. Incorporating supplementary materials can sometimes lead to cost savings. The use of fly ash as partial replacements for cement not only enhances performance but can also be cost-effective. The previous research did studies on the effect of the impact of GO [39–41] on the strength and durability properties. The present study attentions on the combined development of GO and NS with fly ash composites. This investigation will study the influence of GO and colloidal nano-silica with fly ash [43] blended cement composites on mechanical properties, durability properties, and microstructural characteristics. This research focuses on providing sustainable and economical cementitious composite.

2. MATERIALS AND METHODS

2.1. Materials

The constituents used for the study are OPC 53 grade cement, M-Sand, Class F Fly ash, Nano Silica (NS), and Graphene oxide (GO). The major compositions of OPC 53 cement, as per Table 2 of IS 12269:2013 [21], are Silicon dioxide (SiO_2) and Calcium Oxide (CaO). As per Table 2 of ASTM C618 [22], the significant compositions of Class F type fly ash are silicon dioxide (SiO_2), Aluminium oxide (Al_2O_3) and Ferric oxide (Fe_2O_3). Nano silica is composed of Silicon Dioxide (SiO_2). Energy Dispersive X-Rays (EDX) technique is performed to find the composition of Graphene Oxide (GO).

2.2. Material characterization

Fly ash, Nano Silica, and Graphene Oxide are characterized by using a scanning electron microscope (SEM). Using an electron gun, the SEM creates a huge magnified image of a small particle. This aids in determining

the size and structure of nanoscale particles. FA's SEM image is shown in Figure 1. Using ImageJ software, the size of 30 randomly selected particles in the image is calculated. From the 30 particles, the highest size is 73.78×10^{-6} m and smallest is 11.26×10^{-6} m. About $37.52 \mu\text{m}$ average size is used. The standard deviation is 15×10^{-6} m and it is clear that the particle size is not homogeneous. The scatter diagram is depicted in Figure 2. The significance of scatter plots lies in their ability to visually depict the relationship between two variables. The plot had shown the distribution of size of particle that are randomly considered from SEM. This helps in understand the particle size statistically. Figure 2 displays the SEM picture for NS. Using ImageJ software, the size of the nano-silica particle is determined by selecting 30 random particles from the image for measurement. Taking a random particle size in SEM image reading is a methodological choice that enhances the validity, reliability, and generalizability of the results. It ensures that the collected data is representative of the entire sample, contributes to statistical significance, and avoids biases that could arise from non-randomized sampling approaches. These 30 particles range in size from 8.98nm to a maximum of 22.14 nm. 14.274 nm is the average size. The standard deviation is 3.3 nm and confirms size is nearly consistent. The scatter plot is shown in Figure 3.

The image from SEM for GO is presented in Figure 4. The same workout has been performs as above and particle size is measured by means of ImageJ software. Extreme high size from those 30 random particles is 18.064 nm and lowest size is 4.753 nm. Average is 10.01 nm. The GO is almost uniform with as SD is found to be 3.2 nm. The scatter plot of Nano silica is also shown in Figure 3.

Table 2: Chemical composition of fly ash, NS and cement (%).

MATERIAL	LOSS ON IGNITION (LOI)	SiO ₂	CaO	MgO	Fe ₂ O ₃	Al ₂ O ₃
NS	0.73	99.06	–	–	–	–
Cement	2.39	26.47	62.08	1.65	2.74	1.13
Fly ash	2.54	67.42	1.75	0.40	3.80	19.68

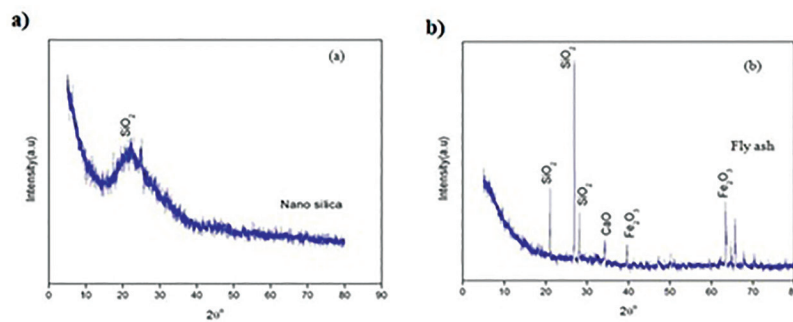


Figure 1: XRD image of (a) nano silica and (b) fly ash.

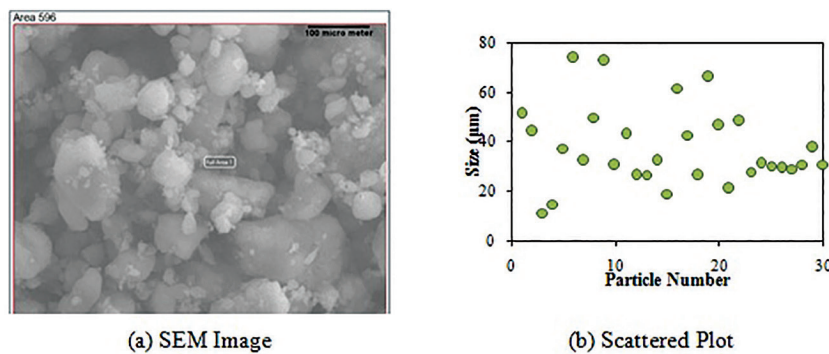


Figure 2: Characterization of Fly Ash a) SEM analysis and b) Scatter plot.

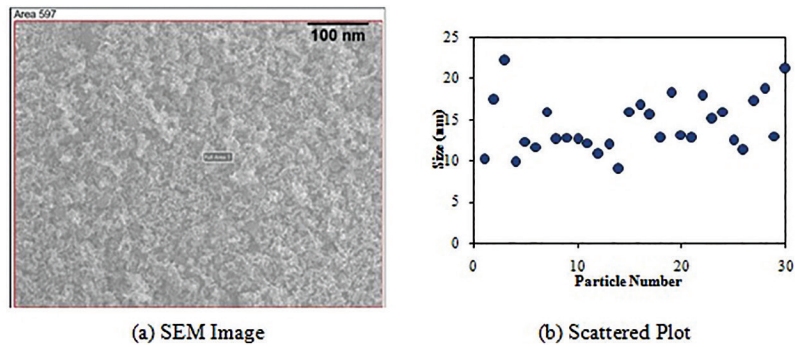


Figure 3: Characterization of Nano Silica a) SEM analysis and b) Scatter plot.

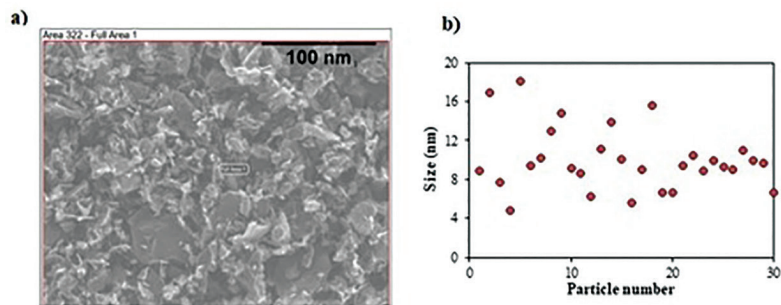


Figure 4: Characterization of GO a) SEM analysis and b) Scatter plot.

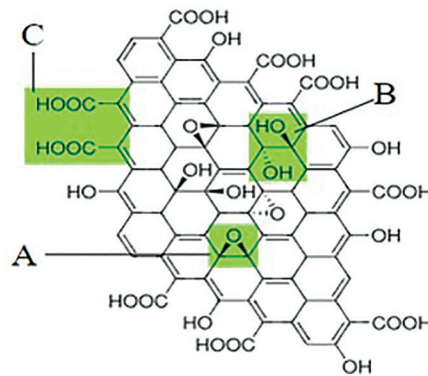


Figure 5: GO Structure Proposed by Heyong *et al.*

GO has oxidizing graphite carbon atoms to preserve the integrity. The $-COOH$, $-OH$ functional groups are located at the lattice position in GO, making significantly higher chemically active material. It does not absorb any visible light and has low electrical conductance (Figure 5).

Energy Dispersive X-Ray (EDX) study is employed for the element compositional study in GO. The essential concept of EDX is that each component has a unique atomic structure that enables a unique collection of peaks on its electromagnetic emission spectrum. The electromagnetic emission spectrum of the EDX is shown in Figure 6. The abscissa in the spectrum is in kilo electron Volts (keV), and the ordinate of the spectrum indicates the intensity. Table 3 shows the elemental composition of GO resulting from EDX analysis. It has been observed that carbon takes the major part, around 94.7%, and oxygen takes the following position with 4.3%. The other elements present in GO are Magnesium, Aluminium, Silica, and Sulphur.

Fourier Transform Infrared Spectroscopy (FTIR) also carried out on GO particles to find the functional groups present in the Specimen. This works on the principle that different functional groups absorb IR radiations

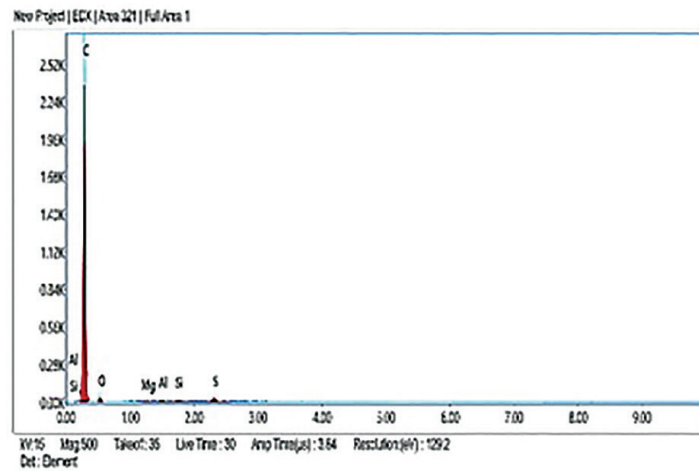


Figure 6: EDX Electromagnetic emission spectrum.

Table 3: Elemental composition of GO.

ELEMENT	C	O	Mg	Al	Si	S
Atomic %	94.7	4.3	0.2	0.2	0.2	0.4

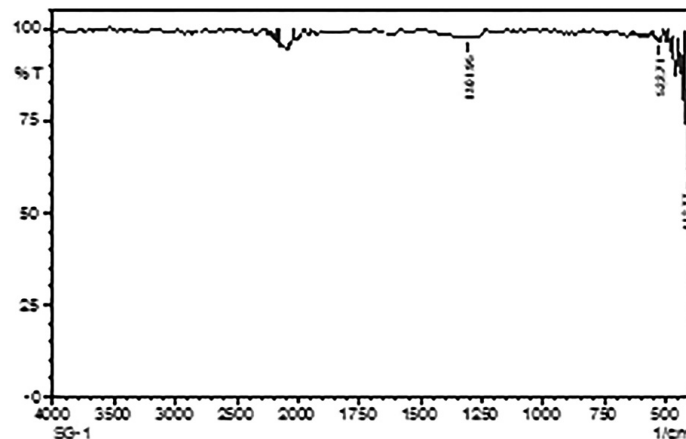


Figure 7: FTIR Spectrum of GO.

at specific frequencies. FTIR spectrum for GO is shown in Figure 7. The X-axis typically represents the wavenumber of the infrared radiation. Wavenumber is the reciprocal of wavelength and is often used in FTIR spectroscopy. It is measured in reciprocal centimetres (cm^{-1}). The wavenumber scale provides information about the energy levels associated with different vibrational modes in the sample. The Y-axis represents the transmittance of the sample at each wavenumber. Transmittance is the ratio of the intensity of transmitted infrared radiation through the sample to the intensity of the incident radiation.

3. EXPERIMENTAL INVESTIGATIONS

3.1. Mortar mix

The study mainly focuses on the incorporation of using Nanomaterials. On the basis of a 10% replacement of cement, the mix proportion was prepared. The different mortar mixes is presented in Table 4. Four mortar mixes are prepared and tested for this investigation. They are cement mortar, cement mortar+FA, cement mortar+FA+NS, and cement mortar+FA+NS+GO. The concentration of Nano Silica in concrete influences

Table 4: Mortar mix proportion.

MIX ID	WATER	CEMENT	M-SAND	FA (% BY wt)	NS (% BY wt)	GO (% BY wt)
	MI	g	g	g	g	g
C	100	200	600	–	–	–
C+FA	100	180	600	20	–	–
C+FA+NS	100	175	600	20	5	–
C+FA+NS+GO0.02	100	175	600	20	5	0.04
C+FA+NS+GO0.03	100	175	600	20	5	0.06
C+FA+NS+GO0.04	100	175	600	20	5	0.08
C+FA+NS+GO0.05	100	175	600	20	5	0.10
C+FA+NS+GO0.06	100	175	600	20	5	0.12

its properties. The choice of 5% concentration is found to provide optimal performance from many existing literatures. A higher concentration provides diminishing results. Hence this has been chosen.

Control mortar composed 100% of OPC as a binder. Next mix composed of 10% fly ash as a fractional replacement to OPC and is labeled as C+FA. The third mix consists of 10% fly ash with 2.5% Nano silica, is used as a fractional replacement for OPC, and is designated as C+FA+NS. The fourth group of the mix is assigned as C+FA+NS+GO. It consists of 10% FA and 2.5% of NS as a fractional replacement to OPC, and GO is used as an additive for the cement. GO of variable proportions 0.02%, 0.03%, 0.04%, 0.05% and 0.06% by weight of cement are used along with FA, NS and represented by C+FA+NS+GO0.02, C+FA+NS+GO0.03, C+FA+NS+GO0.04, C+FA+NS+GO0.05, and C+FA+NS+GO0.06. Before GO is incorporated into the mix, GO, and NS suspension are sonicated [26] separately for 30 minutes in the presence of water. Figure 8 shows the preparation of some specimens.

A homogenous mix of cement, fly ash, and sand, 70% water was mixed dry by hand, and the lasting 30% of the water was used in the diffusion of GO and NS. All mortar specimens are cast in 50 cm² mould and cured. Samples are tested for each category, and hence a total of 72 specimens have been cast. Figure 9 shows the Schematic representation of Cement+FA+GO+NS formation.

3.2. Fluidity of cement paste

The mini flow table test is a widely adopted method for determining the workability of fresh cementitious pastes. This test is carried out to study the effect of colloidal Nano silica, GO and FA on cement-based composites [33–34]. To examine the fluidity of the cement composites, a mini slump cone with the following dimensions is used: 57 mm in height, 38 mm in bottom diameter, and 19 mm in top diameter. The cement paste was poured into the mold in three layers and tamped 25 times using a tamper. Once the mould has been lifted, the sample collapses. The total flow table is raised and dropped 25 times using the lever in the setup. The diameter of the collapsed sample is measured, and the test results are taken from the average of four measurements.

The fluidity of cement pastes for our mix is shown in Figure 10. Incorporation of Nano silica and GO with cement will cause a reduction in fluidity property related to the control cement paste. The flow diameter is gradually reduced with an increase in GO content. On the other hand, adding fly ash with cement will enhance the cement composites' workability. The primary reason for the reduction in the fluidity is the existence of oxygen functional groups and large specific surface area of the Nanoparticles. The large surface area consumes more water for particle lubrication, causing GO particles to absorb a significant amount of water. This, in turn, reduces the quantity of free water within the cement matrix. Interaction between GO with cement releases cationic products, which leads to a reduction in fluidity. The combination of fly ash improves the fluidity of the cement paste since it forms flocculation with cement and improves the cement composite's fluidity. Figure 9 shows the bar chart for the fluidity of cement pastes.

3.3. Compressive strength

Compression tests are conducted for all mortar specimens to find its compressive strength. A total of 72 specimens are tested. Average is presented in Table 5. This value varies within 12% which is well within code limits.

The strength of the fly ash-reinforced cement combinations is reduced compared to the 100% OPC mixed specimens. The highest found at C+FA+NS+GO0.03 mix specimens at all curing ages. After that further

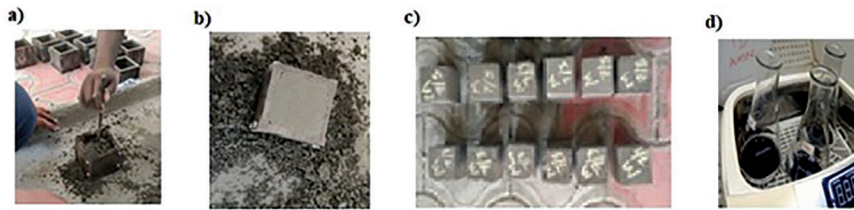


Figure 8: a) Preparation of Specimens, b) Casted Specimen c) Some Prepared Specimen and d) Sonication A homogenous mix of cement, fly ash, and sand, 70% water was mixed dry by hand, and the lasting 30% of the water was used in the diffusion of GO and NS. All mortar specimens are cast in 50 cm² mould and cured. Samples are tested for each category, and hence a total of 72 specimens have been cast. Fig. 8 shows the Schematic representation of Cement + FA + GO + NS formation.

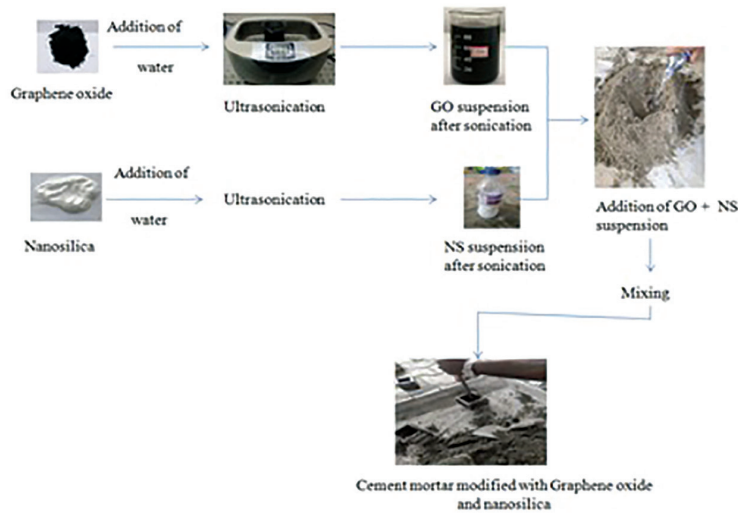


Figure 9: Schematic Representation of Preparation of Mortar.

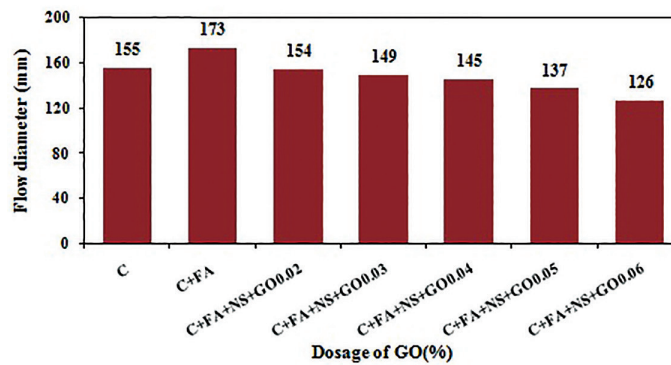


Figure 10: Fluidity of Cement Paste.

Table 5: Strength of mortars.

MIX ID	COMPRESSIVE STRENGTH (MPa)		
	3 DAYS	7 DAYS	28 DAYS
C	23	37	54
C+FA	20	26	35
C+FA+NS+GO0.02	21.72	27.58	36.61
C+FA+NS+GO0.03	29.55	34.75	41.37
C+FA+NS+GO0.04	28.58	33.23	39.15
C+FA+NS+GO0.05	25.32	31.6	38.23
C+FA+NS+GO0.06	23.64	30.43	37.42

increase of GO content will cause a reduction in compressive Strength. Figure 11 indicates the line plot for the strength of cement mortars.

It can be perceived from Figure 11 that that the slope of the control specimen after 7 days of strength is relatively high than other specimens. In other words, the rate of gaining Strength in the cement mortars with the addition of Nanoparticles decreases considerably. Table 6 displays the rise in the Strength for C+FA mix. The maximum increase found to be 47.75%, 33.65%, and 18.20% for C+FA+NS+GO0.03 mix specimens compared to C+FA mix specimens at the end of 3 days, 7 days, and 28days age of curing, respectively.

Incorporating GO into fly ash cement accelerates hydration by promoting subordinate hydration products [27–30]. It is found that GO is adsorbed on the surface of fly ash and cement hydration products due to its large specific surface area. The combination of GO with FA refines the pore structure of the composite [37–38]. The presence of pores and harmful cracks are occupied by excessive CSH gel. This roots compact and dense micro-structure. Figure 12 shows the scatter line plot.

3.4. Water absorption test

This experiment is performed as per ASTM C 642 [24]. The amount of water absorbed is calculated as the code directions and reported in Table 7.

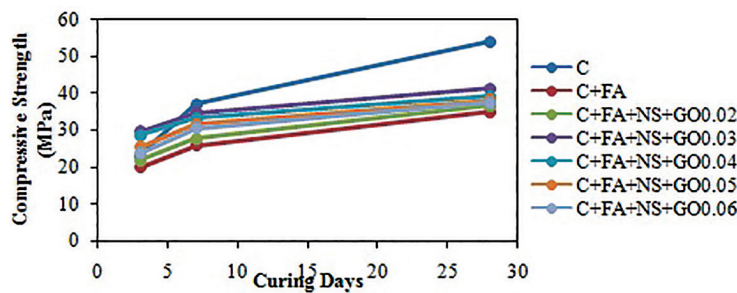


Figure 11: Compressive Strength of Cement Mortars.

Table 6: % increase in strength.

MIX ID	3 DAYS	7 DAYS	28 DAYS
C+FA	–	–	–
C+FA+NS+GO0.02	8.6	6.08	4.6
C+FA+NS+GO0.03	47.75	33.65	18.2
C+FA+NS+GO0.04	31.58	19.23	11.86
C+FA+NS+GO0.05	26.6	17.69	9.23
C+FA+NS+GO0.06	18.2	17.04	6.91

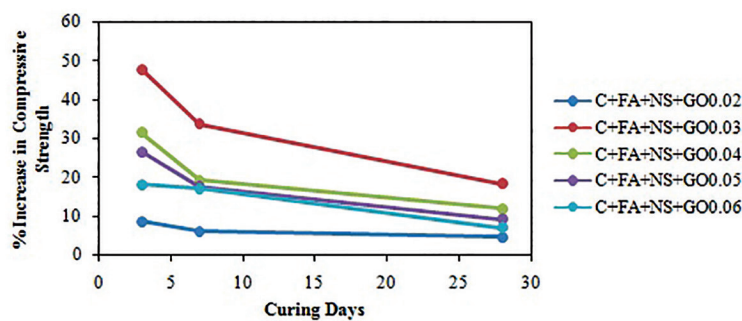


Figure 12: Percentage increase in Compressive Strength.

Table 7: Water absorption by samples (%).

SPECIMEN	WATER ABSORPTION (%)
C	13.43
C+FA	11.5
C+FA+NS+GO0.02	9.32
C+FA+NS+GO0.03	5.92
C+FA+NS+GO0.04	7.74
C+FA+NS+GO0.05	8.03
C+FA+NS+GO0.06	8.65

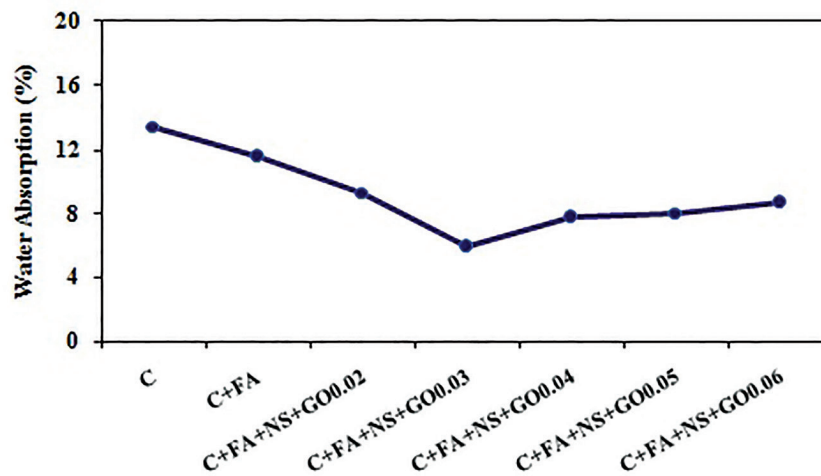


Figure 13: Water Absorption by Mortars.

The water absorption for the specimens C, C+FA, C+FA+NS+GO0.02, C+FA+NS+GO0.03, C+FA+NS+GO0.04, C+FA+NS+GO0.05, C+FA+NS+GO0.06 specimens are 13.43%, 11.5%, 9.32%, 5.92%, 7.74%, 8.03%, 8.65% respectively. The water absorption rate for the GO and NS blended cement composites are less related to the control mortar specimens. This phenomenon happens due to the refinement of pore structure which restrains the entry of water to the inner portion of the composites. This test results shows that the water absorption by cement mortar reduces drastically with the addition of GO. It is also interesting to observe that the water absorption rate decreases up to 0.03% addition of GO and then slightly increases with further addition of GO. As mentioned above, the combination of GO with FA refines the pore structure of the composite. This is also effective to a certain extent, as seen in compressive strength behavior. This is shown as a line scatter plot in Figure 13.

3.5. UPV test

UPV examinations are executed on the mortars for determining quality of the mix as per IS 13311 [25]. Direct transmission method is performed on all six sides of the Specimen. The average value is stated in Table 8. While Ultrasonic Pulse Velocity (UPV) testing is commonly associated with concrete, it can be applied to various construction materials, including mortar. UPV direct transmission makes it suitable for detecting variations in material properties and identifying potential defects or anomalies. UPV direct transmission is relatively simple to perform and can provide results quickly. If the primary goal is to obtain a rapid assessment of the material's condition or quality, direct transmission testing may be a practical and efficient choice.

From Table 2 of IS 13311 [25], designates the velocity standard for grading of quality. The velocities of the control mortar mixes for the all three-curing period are tabulated in Table 8. Almost in all mortar mixes, the quality arrays from good to excellent quality. This is due to the occurrence of fine particles which improves the pore-filling effect which ensures quality and homogeneity. Figure 14 displays the bar chart representing the UPV result.

3.6. Carbonation test

For Further studies, some mortars have been cast with C+FA+NS+GO0.03 mix as it gets more attention over others. Carbonation test has been performed on it to find the extent of carbon dioxide (CO₂) penetration into the Specimen. For performing this Test, the cement mortar specimens are exposed to air for about 28 days and the mortar specimens are split into two halves. A pH indicator 0.2% phenolphthalein is sprayed on two parts of the split mortar specimens. The phenolphthalein indicator reacts with the unhydrated lime content of the specimens and produces anopticalcolour change. The area with colour changes to pink is not affected by carbonation and the area that does not undergo colour change is influenced by carbonation. It has been observed that the depth of carbonation is about a maximum of 3 mm for our Specimen from the free surface, as seen in Figure 15. GO and NS blended cement composites refine the pore structure of the composites, restraints the entry of CO₂. The presence of CO₂ enters into the structural elements will accelerate the corrosion. Nanoparticle blended cement composites fill the pores and cracks present in the composites due to the refinement of microstructure, leads dense and compact structure restraining the entry of CO₂ into the composites.

3.7. Heat resistance

Heat resistance examination [31] performed on C+FA+NS+GO0.03. This stuff is estimated by warming control and C+FA+NS+GO0.03 samples in a furnace at 250°C at the rate 300°C/hr as seen in Figure 16 and left for 1.5 hours for maintaining thermal equilibrium. Then it is cooled for 2 days in room temperature. The same experiment is performed with 500°C and reported in Table 9.

Cement concrete exposed to fire at higher temperature breakdowns the binding stuff of the elements Ca, Si, Al etc., leads failure. Table 9 describes the test results. In Comparison with control specimen, the residual strength of C+FA+NS+GO0.03 are 91.31% higher. The test results show that the residual compressive Strength of C+FA+NS+GO0.03 specimens is more compared to the control specimens subjected to 250°C and 500°C. Figure 17 shows the line scatter plot for the cement mortar at different temperatures.

Table 8: UPV test.

MIX ID	VELOCITY OF ULTRASONIC WAVES (km/s)		
	3 DAYS	7 DAYS	28 DAYS
C	3.2	3.4	4.0
C+FA	3.6	3.8	4.2
C+FA+NS+GO0.02	4.0	4.5	5.0
C+FA+NS+GO0.03	4.2	5.1	4.5
C+FA+NS+GO0.04	5.0	5.2	4.0
C+FA+NS+GO0.05	4.9	5.2	4.6
C+FA+NS+GO0.06	4.2	4.8	5.0

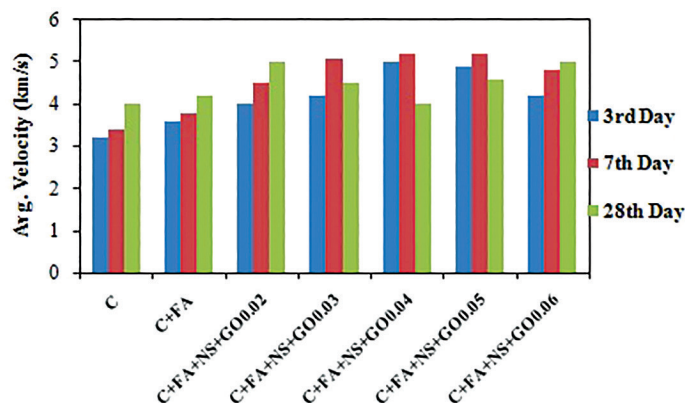


Figure 14: UPV on Mortars.



Figure 15: Carbonation Test.



Figure 16: Heating the Specimen.

Table 9: Mortar strength at various temperatures.

ID	RESIDUAL COMPRESSIVE STRENGTH (MPa)		
	AT ROOM TEMPERATURE	250°C	500°C
C	54	5.76	3.84
C+FA+NS+GO0.03	41.37	11.02	7.87

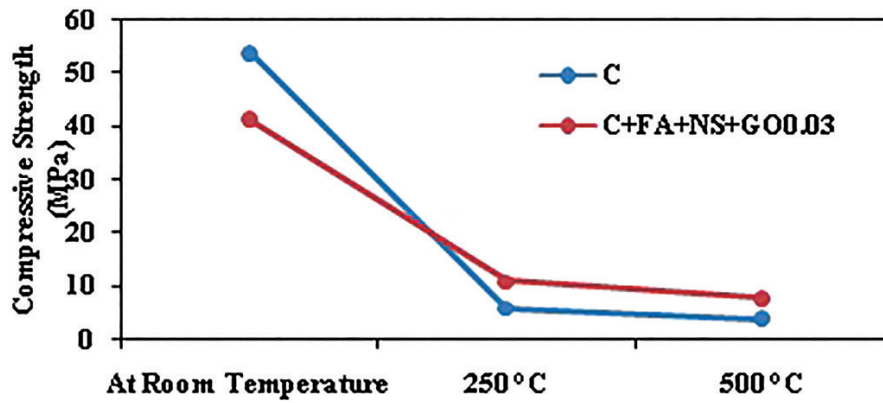


Figure 17: Compressive Strength at Different Temperatures.

3.8. Acid resistance test

Acid resistance examination [32] is used to assess this stuff of the mortars. The two Specimens Control and C+FA+NS+GO0.03 are dipped independently in H₂SO₄ and HCl. 5% HCl and 5% H₂SO₄ are taken separately and specimens are submerged for 28 days. After that, the specimens are taken, washed using distilled water, and dried for 48 hrs and are presented in Table 10.

The strength for control mortar and C+FA+NS+GO0.03 samples are found to be 6.35 MPa and 15.87 MPa. The strength of the specimen after acid immersion of the C+FA+NS+GO0.03 specimen is higher than the control specimen. Similarly, strength after the 5% sulphuric acid immersion are 6.92 MPa, and 13.68 MPa, respectively as seen in Figure 18. The strength after H₂SO₄ immersion test is more than the control specimen. This reduction in the Strength of the control specimen is due to the conversion of calcium compounds into calcium salts, which reduces the Strength. GO, and NS blended cement composites performed better than the control specimens since the Nanoparticles are comparatively stable against chemical exposure.

3.9. Characterization of mortar

The performance of the C+FA+NS+GO0.03 specimen seems good in almost all aspects. The attention over it leads to the study of its characterization using SEM, XRD, EDX, and FTIR. The sample with 7 days of curing has been taken for the study. The mortar has been broken, and the broken samples are collected for analysis.

The SEM images of the control specimen C and specimen C+FA+NS+GO0.03 has been shown in Figure 19. The SEM image of C+FA+NS+GO0.03 specimens shows needle-shaped hydration crystals. The presence of needle-shaped hydration crystals is liable for compressive strength improvement. The development of needle-shaped hydration crystals is due to the presence of oxygen functional groups in GO. Both samples are subjected to Energy Dispersive X-Ray (EDX) Analysis to determine their elemental composition. Figure 20 depicts the electromagnetic emission spectrum of the EDX. The ordinate of the spectrum denotes the intensity, and the abscissa of the spectrum is in kilo electron Volts (keV).

Table 11 shows the EDX test results for the both specimens at 7 days of curing. It shows the elemental percentage composition. The presence of elements such as oxygen (O), magnesium (Mg), calcium (Ca), sulfur (S), silica (Si), aluminum (Al), and iron (Fe) with a percentage composition are shown. The calcium and silicon elements are enhanced in the C+FA+NS+GO0.03 Specimen, which plays a significant role in this improved behavior of the Specimen.

Table 10: Compressive strength of mortar specimen after acid attack.

SPECIMEN ID	RESIDUAL STRENGTH (MPa)		
	ORIGINAL STRENGTH	AFTER 5% Hcl ATTACK	AFTER 5% H ₂ SO ₄ ATTACK
C	54	6.35	6.92
C+FA+NS+GO0.03	41.37	15.87	13.68

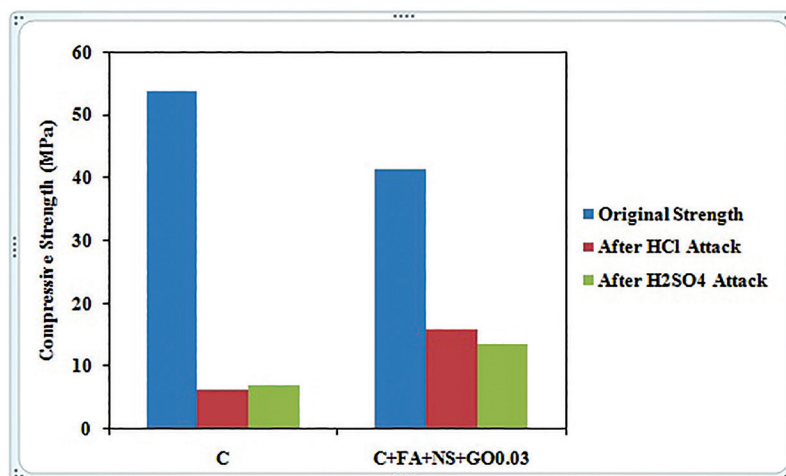


Figure 18: Compressive Strength of Mortar Specimen after Acid Attack.

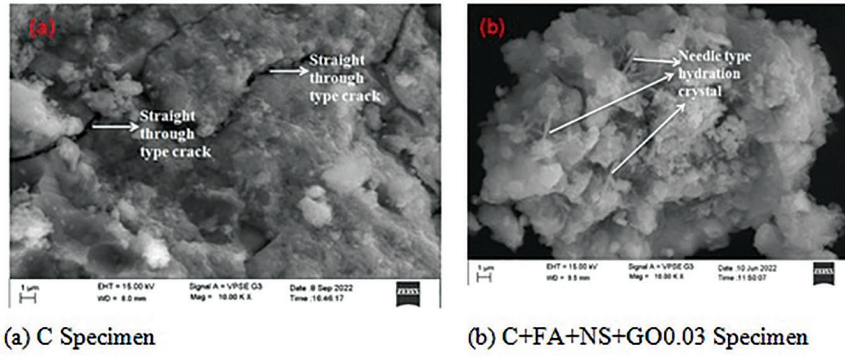


Figure 19: SEM images of Mortars.

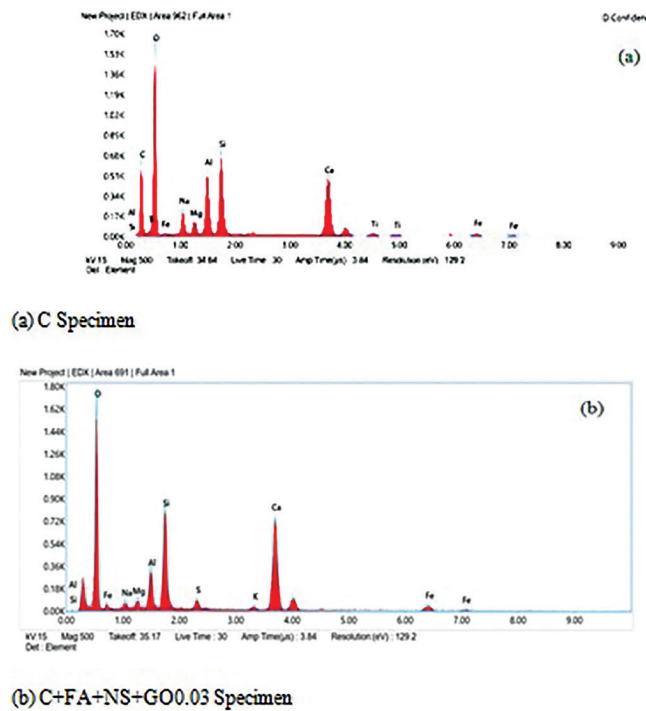


Figure 20: EDX Spectrum of Mortars.

Table 11: EDX analysis on control and C+FA+NS+GO0.03 based cement composite (%).

SPECIMEN	C	Al	Ca	Fe	Na	Mg	O	Si	S
C	14.9	12.6	10.7	0.5	4.3	2.6	38.4	15.6	–
C+FA+NS+GO0.03	6.0	7.6	18.9	1.1	1.7	1.5	41.7	19.6	1.7

A non-destructive method for determining a material’s crystallographic structure, chemical composition, and physical characteristics is X-ray diffraction analysis (XRD). (XRD) is a non-destructive technique for finding material’s crystallographic structure which can be found using the intensities and Bragg’s angle, as shown in Figure 21.

Figure 21 shows the existence of the main crystalline products of ettringite (AFt), portlandite (CH), Tricalcium Aluminate or Celite (C₃A), Dicalcium Silicate or Belite (C₂S), tricalcium silicate or Alite(C₃S) etc. XRD intensity peak diffraction locations between control and NS+GO with FA based cement composite are similar

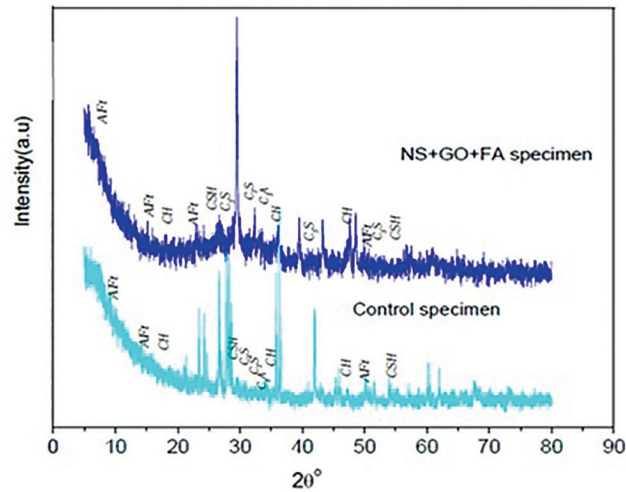


Figure 21: XRD pattern of C and C+FA+NS+GO0.03 cured at 7 days.

Table 12: Phase identification of the specimens.

COMPOUND	ELEMENT NOTATION	2θ ANGLE (C SPECIMEN)	2θ ANGLE (C+FA+NS+G0.03)	CRYSTAL STRUCTURE
Portlandite	CH	18.08, 34.26, 47.18	18.26, 34.16, 47.20	Hexagonal
Jennite	CSH	28.88	28.80	Orthorhombic
Tobermorite	CSH	54.28	54.82	Triclinic
Elite	C3S	29.46,51.8,41.36	29.48,51,41	Triclinic
Belite	C2S	32.2	32.18	Monoclinic
Celite	C3A	32.32	32.32	Isometric
Ettringite	AFt	9.38,15.9,50.01	6.58,15.64,22.14,50.20	Hexagonal

to control. The broad peak in CSH gel in Figure 20 indicates the amorphous nature[42] of the specimens. The diffraction peak positions of crystalline compounds are shown in Table 12.

The crystalline phase change caused by the combination of GO and NS. This alters the microstructure of blended cement composites which results in a more compact and denser microstructure helps in the improvement of the composites compressive Strength and durability.

4. DISCUSSION

Incorporation of Nano silica and GO with cement will cause a reduction in fluidity property related to the control cement paste. The flow diameter is gradually reduced with an increase in GO content. On the other hand, adding fly ash with cement will enhance the cement composites' workability. Graphene oxide has a high specific surface area due to its two-dimensional structure [35]. When added to a mixture, it tends to absorb water, reducing the overall water content available for maintaining fluidity. The water absorption rate for the GO and NS blended cement composites are less related to the control mortar specimens. This phenomenon happens due to the refinement of pore structure which restrains the entry of water to the inner portion of the composites. This test results shows that the water absorption by cement mortar reduces drastically with the addition of GO.

Almost in all mortar mixes, the quality arrays from good to excellent quality. This is due to the occurrence of fine particles which improves the pore-filling effect which ensures quality and homogeneity[36]. It has been observed that the depth of carbonation is about a maximum of 3 mm for our Specimen from the free surface. In Comparison with control specimen, the residual strength of C+FA+NS+GO0.03 is 91.31% higher for temperature test. The strength for control mortar and C+FA+NS+GO0.03 samples are found to be 6.35 MPa and 15.87 MPa. The strength of the specimen after acid immersion of the C+FA+NS+GO0.03 specimen is higher than the control specimen. Similarly, strength after the 5% sulphuric acid immersion are 6.92 MPa, and 13.68 MPa, respectively. The crystalline phase change caused by the combination of GO and NS.

This alters the microstructure of blended cement composites which results in a more compact and denser microstructure helps in the improvement of the composites compressive Strength , durability and flexural properst as well [44].

5. CONCLUSION

The detailed experimental investigations are performed on GO blended cement matrix. From the previous studies, the work has been enhanced with the inclusion of Nano silica and fly ash. This combined effect of Fly ash, Cement, Nano silica and GO C+FA+NS+GO0.03 mix enhances the overall mechanical behavior. Both Fresh and hardened properties are admirable for the mix. Hardened properties are enhanced in good extent. The following conclusions are drawn based on the experiments. Compressive Strength of NS and GO blended cement composites are higher than that of the control specimen. This is because of the refined micro structure of cement mortars by Nano materials. This is illustrated by SEM images and the presence of needle like hydration crystal enhances the dense and compact microstructure.

- Presence of hydrophilic groups and huge specific surface area of the NS and GO particles causes reduction in fluidity of the cement compound with rise in content of GO and NS.
- XRD results reveal that GO act as a seeding compound in cement pore solution accelerates the growth of CSH and other hydration products.
- EDX analysis shows that the existence of calcium and silicon elements enhances the overall behaviour of the composite.
- The material performance study should be prolonged to find the structural performances such as Bending, Shear and Compression.

6. ACKNOWLEDGEMENT

I am deeply indebted to Government college of Engineering, Salem, Tamil Nadu, India where all the experimental work has been carried out. I would like to express my deepest thankfulness to Photonics Lab, Sona College of Technology, Salem, Tamil Nadu where I have sonicated my Nano particles. I would like to extend my Thankful to Vignanabhavana Institute of excellence, University of Mysore, Karnataka, India who supported for all micro structural characterization tests.

7. BIBLIOGRAPHY

- [1] SHAMSAEI, E., SOUZA, F.B., YAO, X., *et al.*, “Graphene-based nano sheets for stronger and more durable concrete: a review”, *Construction & Building Materials*, v. 183, pp. 642–660, 2018. doi: <http://dx.doi.org/10.1016/j.conbuildmat.2018.06.201>.
- [2] LIN, Y., DU, H., “Graphene reinforced cement composites: a review”, *Construction & Building Materials*, v. 265, pp. 120312, 2020. doi: <http://dx.doi.org/10.1016/j.conbuildmat.2020.120312>.
- [3] LV, S., LIU, J., SUN, T., *et al.*, “Effect of GO nano sheets on shapes of cement hydration crystals and their formation process”, *Construction & Building Materials*, v. 64, pp. 231–239, 2014. doi: <http://dx.doi.org/10.1016/j.conbuildmat.2014.04.061>.
- [4] KANG, X., ZHU, X., QIAN, J., *et al.*, “Effect of graphene oxide (GO) on hydration of tricalcium silicate (C₃S)”, *Construction & Building Materials*, v. 203, pp. 514–524, 2019. doi: <http://dx.doi.org/10.1016/j.conbuildmat.2019.01.117>.
- [5] CHINTALAPUDI, K., PANNEM, R.M.R., “The effects of Graphene Oxide addition on hydration process, crystal shapes, and microstructural transformation of Ordinary Portland Cement”, *Journal of Building Engineering*, v. 32, pp. 101551, 2020. doi: <http://dx.doi.org/10.1016/j.job.2020.101551>.
- [6] LI, W., LI, X., CHEN, S.J., *et al.*, “Effects of graphene oxide on early-age hydration and electrical resistivity of Portland cement paste”, *Construction & Building Materials*, v. 136, pp. 506–514, 2017. doi: <http://dx.doi.org/10.1016/j.conbuildmat.2017.01.066>.
- [7] LV, S., LIU, J., SUN, T., *et al.*, “Effect of GO nanosheets on shapes of cement hydration crystals and their formation process”, *Construction & Building Materials*, v. 64, pp. 231–239, 2014. doi: <http://dx.doi.org/10.1016/j.conbuildmat.2014.04.061>.
- [8] SHANG, Y., ZHANG, D., YANG, C., *et al.*, “Effect of graphene oxide on the rheological properties of cement pastes”, *Construction & Building Materials*, v. 96, pp. 20–28, 2015. doi: <http://dx.doi.org/10.1016/j.conbuildmat.2015.07.181>.

- [9] LI, X., LU, Z., CHUAH, S., *et al.*, “Effects of graphene oxide aggregates on hydration degree, sorptivity, and tensile splitting strength of cement paste”, *Composites. Part A, Applied Science and Manufacturing*, v. 100, pp. 1–8, 2017. doi: <http://dx.doi.org/10.1016/j.compositesa.2017.05.002>.
- [10] PAN, Z., HE, L., QIU, L., *et al.*, “Mechanical properties and microstructure of a graphene oxide-cement composite”, *Cement and Concrete Composites*, v. 58, pp. 140–147, 2015. doi: <http://dx.doi.org/10.1016/j.cemconcomp.2015.02.001>.
- [11] ALEX, G., KEDIR, A., TEWELE, T.G., “Review on effects of graphene oxide on mechanical and microstructure of cement-based materials”, *Construction & Building Materials*, v. 360, pp. 129609, 2022. doi: <http://dx.doi.org/10.1016/j.conbuildmat.2022.129609>.
- [12] WU, L., XIE, Z., GU, L., *et al.*, “Investigation of the tribological behavior of graphene oxide nanoplates as lubricant additives for ceramic/steel contact”, *Tribology International*, v. 128, pp. 113–120, 2018. doi: <http://dx.doi.org/10.1016/j.triboint.2018.07.027>.
- [13] WĘGIEL, J., BURDAT, B., SKRZYPEK, S., “A graphene oxide modified carbon ceramic electrode for voltammetric determination of gallic acid”, *Diamond and Related Materials*, v. 88, pp. 137–143, 2018. doi: <http://dx.doi.org/10.1016/j.diamond.2018.07.012>.
- [14] BASQUIROTO DE SOUZA, F., SHAMSAEI, E., SAGOE-CRENTSIL, K., *et al.*, “Proposed mechanism for the enhanced microstructure of graphene oxide–Portland cement composites”, *Journal of Building Engineering*, v. 54, pp. 104604, 2022. doi: <http://dx.doi.org/10.1016/j.jobe.2022.104604>.
- [15] SHARMA, S., SUSAN, D., KOTHIYAL, N.C., *et al.*, “Graphene oxide prepared from mechanically milled graphite: Effect on strength of novel fly-ash based cementitious matrix”, *Construction & Building Materials*, v. 177, pp. 10–22, 2018. doi: <http://dx.doi.org/10.1016/j.conbuildmat.2018.05.051>.
- [16] WANG, Q., CUI, X., WANG, J., *et al.*, “Effect of fly ash on rheological properties of graphene oxide cement paste”, *Construction & Building Materials*, v. 138, pp. 35–44, 2017. doi: <http://dx.doi.org/10.1016/j.conbuildmat.2017.01.126>.
- [17] PRABAVATHY, S., JEYASUBRAMANIAN, K., PRASANTH, S., *et al.*, “Enhancement in behavioral properties of cement mortar cubes admixed with reduced graphene oxide”, *Journal of Building Engineering*, v. 28, pp. 101082, 2020. doi: <http://dx.doi.org/10.1016/j.jobe.2019.101082>.
- [18] LEE, S.J., JEONG, S.H., KIM, D.U., *et al.*, “Effects of graphene oxide on pore structure and mechanical properties of cementitious composites”, *Composite Structures*, v. 234, pp. 111709, 2020. doi: <http://dx.doi.org/10.1016/j.compstruct.2019.111709>.
- [19] LI, X., LIU, Y.M., LI, W.G., *et al.*, “Effects of graphene oxide agglomerates on workability, hydration, microstructure and compressive strength of cement paste”, *Construction & Building Materials*, v. 145, pp. 402–410, 2017. doi: <http://dx.doi.org/10.1016/j.conbuildmat.2017.04.058>.
- [20] WANG, Q., LI, S., PAN, S., *et al.*, “Effect of graphene oxide on the hydration and microstructure of fly ash-cement system”, *Construction & Building Materials*, v. 198, pp. 106–119, 2019. doi: <http://dx.doi.org/10.1016/j.conbuildmat.2018.11.199>.
- [21] INDIAN STANDARDS, *IS 12269:2013 – Ordinary Portland Cement, 53 Grade – Specification*, New Delhi, IS, 2013.
- [22] AMERICAN SOCIETY FOR TESTING AND MATERIALS, *ASTM C618 – Standard Specification for Coal Fly Ash and Raw or Calcined Natural Pozzolan for Use in Concrete*, West Conshohocken, ASTM, 2022.
- [23] HE, H., KLINOWSKI, J., FORSTER, M., *et al.*, “A new structural model for graphite oxide”, *Chemical Physics Letters*, v. 287, n. 1, pp. 53–56, 1998. doi: [http://dx.doi.org/10.1016/S0009-2614\(98\)00144-4](http://dx.doi.org/10.1016/S0009-2614(98)00144-4).
- [24] AMERICAN SOCIETY FOR TESTING AND MATERIALS, *ASTM C642 – Density, Absorption, and Voids in Hardened Concrete*, West Conshohocken, ASTM, pp. 1–3, 2005.
- [25] BUREAU OF INDIAN STANDARDS, *IS 13311 (Part 1) – Method of Non-Destructive Testing of Concrete, Part 1: Ultrasonic Pulse Velocity*, New Delhi, Bureau of Indian Standards, pp. 1-7, 1992.
- [26] HORSZCZARUK, E., MIJOWSKA, E., KALENCZUK, R.J., *et al.*, “Nanocomposite of cement/graphene oxide - Impact on hydration kinetics and Young’s modulus”, *Construction & Building Materials*, v. 78, pp. 234–242, 2015. doi: <http://dx.doi.org/10.1016/j.conbuildmat.2014.12.009>.
- [27] DEVI, S.C., KHAN, R.A., “Compressive strength and durability behavior of graphene oxide reinforced concrete composites containing recycled concrete aggregate”, *Journal of Building Engineering*, v. 32, pp. 101800, 2020. doi: <http://dx.doi.org/10.1016/j.jobe.2020.101800>.

- [28] LU, Z., LI, X., HANIF, A., *et al.*, “Early-age interaction mechanism between the graphene oxide and cement hydrates”, *Construction & Building Materials*, v. 152, pp. 232–239, 2017. doi: <http://dx.doi.org/10.1016/j.conbuildmat.2017.06.176>.
- [29] LV, S., MA, Y., QIU, C., *et al.*, “Effect of graphene oxide nanosheets of microstructure and mechanical properties of cement composites”, *Construction & Building Materials*, v. 49, pp. 121–127, 2013. doi: <http://dx.doi.org/10.1016/j.conbuildmat.2013.08.022>.
- [30] LI, X., KORAYEM, A.H., LI, C., *et al.*, “Incorporation of graphene oxide and silica fume into cement paste: a study of dispersion and compressive strength”, *Construction & Building Materials*, v. 123, pp. 327–335, 2016. doi: <http://dx.doi.org/10.1016/j.conbuildmat.2016.07.022>.
- [31] CHU, H., JIANG, J., SUN, W., *et al.*, “Effects of graphenesulfonatenanosheets on mechanical and thermal properties of sacrificial concrete during high temperature exposure”, *Cement and Concrete Composites*, v. 82, pp. 252–264, 2017. doi: <http://dx.doi.org/10.1016/j.cemconcomp.2017.06.007>.
- [32] SATA, V., SATHONSAOWAPHAK, A., CHINDAPRASIRT, P., “Resistance of lignite bottom ash geopolymer mortar to sulfate and sulfuric acid attack”, *Cement and Concrete Composites*, v. 34, n. 5, pp. 700–708, 2012. doi: <http://dx.doi.org/10.1016/j.cemconcomp.2012.01.010>.
- [33] LEE, S.J., JEONG, S.H., KIM, D.U., *et al.*, “Graphene oxide as an additive to enhance the strength of cementitious composites”, *Composite Structures*, v. 242, pp. 112154, 2020. doi: <http://dx.doi.org/10.1016/j.compstruct.2020.112154>.
- [34] SUI, Y., LIU, S., OU, C., *et al.*, “Experimental investigation for the influence of graphene oxide on properties of the cement-waste concrete powder composite”, *Construction & Building Materials*, v. 276, pp. 122229, 2021. doi: <http://dx.doi.org/10.1016/j.conbuildmat.2020.122229>.
- [35] INDUKURI, C.S.R., NERELLA, R., MADDURU, S.R.C., “Effect of graphene oxide on microstructure and strengthened properties of fly ash and silica fume based cement composites”, *Construction & Building Materials*, v. 229, pp. 116863, 2019. doi: <http://dx.doi.org/10.1016/j.conbuildmat.2019.116863>.
- [36] ZHANG, Y.R., KONG, X.M., LU, Z.C., *et al.*, “Influence of triethanolamine on the hydration product of portlandite in cement paste and the mechanism”, *Cement and Concrete Research*, v. 87, pp. 64–76, 2016. doi: <http://dx.doi.org/10.1016/j.cemconres.2016.05.009>.
- [37] ANWAR, B.S., MOHAMMED, B.S., WAHAB, M.A., *et al.*, “Enhanced properties of cementitious composite tailored with graphene oxide nanomaterial: a review”, *Developments in the Built Environment*, v. 1, pp. 100002, 2020. doi: <http://dx.doi.org/10.1016/j.dibe.2019.100002>.
- [38] CHUAH, S., PAN, Z., SANJAYAN, J.G., *et al.*, “Nano reinforced cement and concrete composites and new perspective from graphene oxide”, *Construction & Building Materials*, v. 73, pp. 113–124, 2014. doi: <http://dx.doi.org/10.1016/j.conbuildmat.2014.09.040>.
- [39] AN, J., NAM, B.H., ALHARBI, Y., *et al.*, “Edge-oxidized graphene oxide (EOGO) in cement composites: Cement hydration and microstructure”, *Composites. Part B, Engineering*, v. 173, pp. 106795, 2019. doi: <http://dx.doi.org/10.1016/j.compositesb.2019.05.006>.
- [40] PRABAVATHY, S., JEYASUBRAMANIAN, K., PRASANTH, S., *et al.*, “Enhancement in behavioral properties of cement mortar cubes admixed with reduced graphene oxide”, *Journal of Building Engineering*, v. 28, pp. 101082, 2020. doi: <http://dx.doi.org/10.1016/j.jobe.2019.101082>.
- [41] DEVI, S.C., KHAN, R.A., “Effect of graphene oxide on mechanical and durability performance of concrete”, *Journal of Building Engineering*, v. 27, pp. 101007, 2020. doi: <http://dx.doi.org/10.1016/j.jobe.2019.101007>.
- [42] STUTZMAN, P.E., BULLARD, J.W., FENG, P., “Phase analysis of portland cement by combined quantitative X-ray powder diffraction and scanning electron microscopy”, *Journal of Research of the National Institute of Standards and Technology*, v. 121, pp. 47–107, 2016. doi: <http://dx.doi.org/10.6028/jres.121.004>. PubMed PMID: 34434615.
- [43] GANAPATHY, G.P., ALAGU, A., RAMACHANDRAN, S., *et al.*, “Effects of fly ash and silica fume on alkalinity, strength and planting characteristics of vegetation porous concrete”, *Journal of Materials Research and Technology*, v. 24, pp. 5347–5360, 2023. doi: <http://dx.doi.org/10.1016/j.jmrt.2023.04.029>.
- [44] VERAPATHRAN, M., VIVEK, S., ARUNKUMAR, G.E., *et al.*, “Flexural behaviour of HPC beams with steel slag aggregate”, *Journal of Ceramic Processing Research*, v. 24, n. 1, pp. 89–97, 2023.
- [45] KRISHNARAJA, R., KULANTHAIVEL, P., RAMSHANKAR, P., *et al.*, “Performance of polyvinyl alcohol and polypropylene fibers under simulated cementitious composites pore solution”, *Advances in Materials Science and Engineering*, v. 22, pp. 9669803, 2022. doi: <http://dx.doi.org/10.1155/2022/9669803>.